Angular and energy distributions of ^{24}Na fragments formed by the reaction of 11.5-GeV protons with ^{197}Au

J. A. Urbon, S. B. Kaufman, D. J. Henderson, and E. P. Steinberg
Chemistry Division, Argonne National Laboratory, Argonne, Illinois 60439
(Received 17 October 1979)

The angular distribution and the range distributions at three angles have been measured for the light nuclear fragment ^{24}Na formed by the interaction of 11.5-GeV protons with ^{197}Au. The angular distribution has a peak at a laboratory angle $\theta_L = 70°$ and is thus quite different from the forward-peaked angular distribution previously observed for ^{24}Na at a bombarding energy of 2.9 GeV. The velocity distributions derived from the range distributions are relatively narrow, and the mean velocity decreases from 2.11 $(\mathrm{MeV}/A)^{1/2}$ at $\theta_L = 30°$ to 1.86 $(\mathrm{MeV}/A)^{1/2}$ at 156.5°. The data are analyzed in terms of the two-step model of nuclear reactions and are found to be consistent with that model. The model parameters derived from this analysis are $\langle v_\parallel \rangle = 0.14$ $(\mathrm{MeV}/A)^{1/2}$ and $\langle V \rangle = 2.00$ $(\mathrm{MeV}/A)^{1/2}$. The angular distribution in the frame moving with the velocity $v_\parallel$ is found to be symmetric about 90°, with an intensity ratio $I(90°)/I(0°) = 1.43$. The implications of this analysis for the reaction mechanism are discussed.

[NUCLEAR REACTIONS ^{197}Au$(p,x)^{24}$Na, E_p =11.5 GeV; measured angular distribution and range distributions at 30°, 90°, and 156.5°; inferred parameters of two-step model.]

I. INTRODUCTION

The energy spectra and angular distributions of light nuclear fragments emitted from heavy targets under bombardment by energetic protons have been extensively studied. The first such study was that of Cumming *et al.*[1] and was a radiochemical measurement of ^{24}Na formed in the interaction of 2.9-GeV protons with Bi. It was found that the laboratory angular distribution was strongly peaked in the forward (beam) direction and that the energy spectra exhibited a characteristic kinematic shift such as would be due to emission of the fragments in a moving system. The data were analyzed in terms of a two-step model. The first step, arising from a fast intranuclear cascade, results in an excited nucleus moving in the beam direction. In the second step this nucleus then emits the light fragment or its precursor with some distribution of kinetic energy and emission angle in the moving frame. Transformation of the observed laboratory distributions to the moving system yields the pertinent parameters of the process.

If the second step occurred sufficiently slowly that memory (except for angular momentum) of the first step had been lost, the angular distribution in the moving frame should be symmetric about 90° to the beam direction. However, it was not possible to fit the experimental data with a single energy distribution and a symmetric angular distribution in a moving frame. If a symmetric angular distribution was chosen, it would require ^{24}Na nuclei emitted at backward angles to have higher mean kinetic energies than those emitted at forward angles, which seems unlikely. On the other hand, requiring a single energy distribution independent of emission angle led to a forward-peaked angular distribution in the moving frame. It was therefore concluded that the data were incompatible with the assumptions of the model and that the mechanism of fragmentation is a fast process in which memory of the incident projectile direction is retained.

Subsequent studies[2-5] of fragment emission induced by 5–6-GeV protons using on-line counter techniques confirmed these results and showed that they were generally applicable for a wide range of fragment masses and atomic numbers. The data could be described[5] fairly well for heavy targets by a model which assumed isotropic emission of fragments in a two-body breakup process occurring in a moving frame. The energy spectrum in that frame was taken to be a Maxwellian distribution with a Coulomb barrier and an appreciable amount of smearing in order to reproduce the experimental spectral widths. The Coulomb barrier required is only about one-half that calculated for two-body breakup, assuming tangent spheres. However, the experimental angular distributions are more forward peaked than the model predicts, which again suggests that the angular distributions in the moving frame are forward peaked.

A striking change in this pattern of forward-peaked fragments was found by Remsberg and

Perry[6] in the reactions of 28-GeV protons with Au and U. The laboratory angular distributions of $Z = 6-12$ fragments were sideward peaked ($\theta_L \approx 70°$), with the peak shifting forward and becoming less distinct for lower Z fragments. These distributions were essentially identical for the two targets, showing that the phenomenon was a general one, and not dependent on the specific target or fragment within broad limits.

The change in angular distribution with bombarding energy was further demonstrated[7] for the isotopes of Sc ($Z = 21$) formed by bombardment of uranium by protons. At a proton energy of 0.8 GeV the angular distribution was forward peaked, but had changed to one peaked at 90° in the laboratory at 11.5 GeV. Recent measurements[8] with 400-GeV protons of the angular distributions of isotopes of Mg, Sc, Cu, Ag, and Ba formed from uranium show that all products have peaks close to 90°. More unusual, the Sc isotopes and the neutron-deficient Cu and Ag isotopes exhibit a net backward enhancement. That is, the integrated distribution in the backward hemisphere is larger than that in the forward hemisphere.

These changes with bombarding energy are also shown by the thick-target, thick-catcher recoil measurement technique, which measures a range-weighted integral forward-to-backward (F/B) ratio. Measurements on a variety of products from heavy-element targets[9-13] have shown that the F/B ratio increases with bombarding energy up to about 3 GeV, beyond which it decreases.

The question is thus raised whether an analysis similar to that of Ref. 1 of the energy and angular distributions obtained at higher bombarding energies, would give satisfactory agreement with the assumption of the two-step model, i.e., an angular distribution symmetric about 90° in the moving frame. The present work was undertaken to answer this question by making such measurements for ^{24}Na formed in 11.5-GeV proton bombardment of Au.

II. EXPERIMENTAL

The targets were bombarded with 11.5-GeV protons in the internal beam of the Argonne National Laboratory zero-gradient synchrotron (ZGS). They consisted of a thin (140–170 μg/cm^2) layer of Au metal evaporated onto a 0.9 mg/cm^2 Mylar film. The targets were mounted at 30° to the beam in a holder which included a recoil-catcher assembly in a cylindrical geometry with respect to the target. A description of this target holder, as well as the procedure by which the solid angles subtended by the catcher foils were calculated, has been previously published.[14] In order to prevent ^{24}Na recoils generated by spallation reactions in the aluminum holder from interfering, it was sprayed with a plastic coating.

For the angular distribution measurements the catchers were Mylar foils of thickness 18 mg/cm^2, sufficient to stop essentially all of the recoils. Three catcher layers were used, with the second serving as an activation blank and the third as a guard from the aluminum holder. The angular distribution was measured separately for forward and backward angles, with the target reversed for the latter measurements.

Irradiations lasted for 30–60 min at beam intensities of $4-6 \times 10^{11}$ protons/pulse, with a repetition rate of about 4 sec. At intensities approaching 10^{12} protons/pulse the target showed signs of deterioration. The target holder assembly was kept in a retracted position during the acceleration period, in order to protect it from protons below the full energy. It was then flipped up and the 11.5-GeV beam was steered onto the target by the RF program. An aluminum beam bumper protected the catcher foils from exposure to the direct beam.

Following the irradiation the foils were cut into segments of 15° angular width; the angular ranges were 30°–105° (forward) and 75°–150° (backward), giving three points centered at 90° to permit normalization of the two sets of measurements. The Mylar catcher and activation blank foils were dissolved in acid (a 1 : 1 : 0.5 mixture of $H_2SO_4 : HClO_4 : HNO_3$) in the presence of ^{22}Na tracer, which was used to determine the chemical yields. The solutions were boiled to near dryness and the residue dissolved in HCl, and 0.2 g of hydrated antimony pentoxide (HAP)[15] added. This material quantitatively adsorbs sodium in the presence of HCl. Purification consisted of washing the solid with HCl three times, followed by one wash with distilled water. The purified material was counted in a large (12.5 cm × 12.5 cm) NaI (Tl) well crystal, with a lower discriminator set at 2.5 MeV, thus allowing the 2.75-MeV peak and the 4.12-MeV sum peak of ^{24}Na to be counted, with a total efficiency for ^{24}Na of 14%. The activation blanks had <1% of the activity in the catchers. The chemical yields, determined by measurement of the recovery of the ^{22}Na tracer, were 85%–98%.

For the differential range measurements, the same target-catcher holder was used, but the catchers were a stack of thin (300–900 μg/cm^2) Mylar foils covered with an angle-defining mask of thick Mylar. Measurements were made at mean angles of 30°, 90°, and 156.5° with respect to the beam; the angular acceptance was ±15° for the 30° and 90° measurements and ±7.5° at 156.5°. The irradiation conditions, chemical separations, and

counting were done in the same manner as described above.

The data from the angular distribution experiments were corrected for chemical yield and solid angle, and the separate forward and backward measurements combined at their overlapping points, normalizing to a value of unity at 90°. The possible effect of target thickness on the data was investigated by using a 530-μg/cm^2 target to measure the angular distribution. No systematic differences were detected between the two measurements and we conclude that scattering of the ^{24}Na recoils does not distort the results.

The range distributions were corrected for two experimental effects. By using a Mylar foil target of the same thickness as that used for the target backing, it was found that there was an unaccounted for background of ^{24}Na recoils, most of which were stopped in the first catcher foil. This background led to a 30% correction to the intensity of the first catcher foil, but <2% to that of succeeding foils. The second correction was for the spread in path length of the recoils through the catchers due to the fairly large solid angle subtended which, on the average, increased the effective thickness of each foil. This correction varied from 4% for the 30° and 156.5° measurements to 10% for the 90° measurement.

III. RESULTS

The experimental angular distribution as a function of the laboratory angle θ_L with respect to the beam direction is given in Table I; it is normalized to unity at $\theta_L = 90°$. The errors shown are the standard deviations and are compounded from the counting statistics (3–5%) and the estimated uncertainties in chemical yields (2%) and solid angle calculation (2%). The results from the two different target thicknesses were averaged to obtain the data. These data are shown in Fig. 1 as a function of laboratory angle. The solid curve in Fig. 1 shows the calculated angular distribution based on the two-step model, described in the following section. For comparison with the present data, the angular distribution for ^{24}Na from Bi at 2.9 GeV, from Ref. 1, is shown as the dashed curve.

TABLE I. Angular distribution in the laboratory of ^{24}Na formed from Au by 11.5-GeV protons. The data are normalized to unity at 90°.

Laboratory angle θ_L (deg)	Intensity per unit solid angle (arb. units)
30	0.879 ± 0.018
45	0.958 ± 0.020
60	1.010 ± 0.022
75	1.032 ± 0.018
90	1.000
105	0.935 ± 0.015
120	0.831 ± 0.020
135	0.760 ± 0.018
150	0.695 ± 0.022

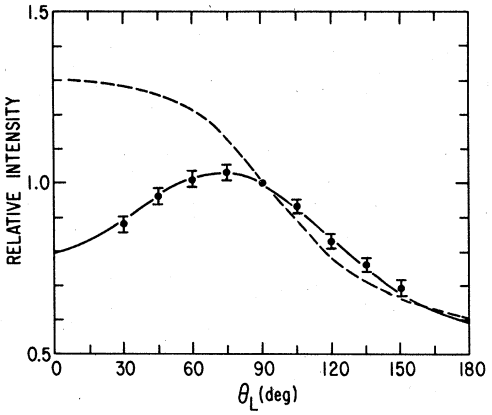

FIG. 1. Angular distribution in the laboratory for ^{24}Na. The data are in units of intensity per unit solid angle, relative to the intensity at 90°. The solid curve is the calculated angular distribution based on the two-step model (see text). The dashed curve shows the angular distribution measured at a bombarding energy of 2.9 GeV (Ref. 1).

The striking difference between these two angular distributions is the change from a strongly forward-peaked one at 2.9 GeV to a sideward-peaked one at 11.5 GeV, where the most probable emission angle is $\theta_L \approx 70°$. As discussed in the Introduction, this type of change is a rather general phenomenon dependent on the incident proton energy, and does not depend on the specific target or fragment within certain limits. Thus the comparison of the present data with a Au target and the 2.9-GeV data with a Bi target is a meaningful one.

The range distributions, corrected as described in the previous section, are given in Table II. Because of the large uncertainty in the activation blank correction for the first foil, it is not included in Table II; thus the first range interval starts at ~0.37 mg/cm^2. This is equivalent to the thickness of the first catcher plus one-half the effective target thickness, converted from Au to Mylar equivalent using range-energy tables.[16] The range distributions were converted to energy and velocity distributions using the Northcliffe-Schilling tables.[16] The kinetic energy distribution at 90° to the beam is shown in Fig. 2 as the full histogram; for comparison the dashed histogram shows the corresponding distribution at 2.9 GeV

TABLE II. ^{24}Na differential ranges in Mylar produced by 11.5-GeV protons on Au.

Angle with respect to beam					
30°		90°		156.5°	
Range interval (mg/cm^2)	Activity fraction[a] per (mg/cm^2)	Range interval (mg/cm^2)	Activity fraction[a] per (mg/cm^2)	Range interval (mg/cm^2)	Activity fraction[a] per (mg/cm^2)
0.372–1.839	0.144 ±0.079	0.378–1.898	0.138 ±0.080	0.370–1.294	0.138 ±0.032
1.839–2.782	0.176 ±0.014	1.898–2.836	0.230 ±0.011	1.294–2.211	0.230 ±0.018
2.782–3.703	0.205 ±0.015	2.836–3.814	$0.236 \pm 0.011_5$	2.211–3.118	0.233 ±0.010
3.703–4.708	0.171 ±0.007	3.814–4.833	$0.174 \pm 0.008_3$	3.118–4.048	0.193 ±0.009
4.708–5.750	$0.128 \pm 0.007_1$	4.833–5.792	$0.104 \pm 0.006_9$	4.048–5.078	0.110 ±0.005
5.750–6.676	$0.084_4 \pm 0.006_3$	5.792–6.809	$0.057_2 \pm 0.005_9$	5.078–6.057	$0.054_7 \pm 0.003$
6.676–7.686	$0.049_1 \pm 0.005_2$	6.809–7.823	$0.035_2 \pm 0.004_7$	6.057–6.968	$0.027_3 \pm 0.002$
7.686–8.755	$0.029_7 \pm 0.004_4$	7.823–8.793	$0.016_1 \pm 0.004_7$	6.968–7.966	$0.010_5 \pm 0.001$
8.755–9.690	$0.013_6 \pm 0.004_9$	8.793–9.771	$0.011_1 \pm 0.004_3$	7.966–9.834	$0.004_2 \pm 0.001$

[a] Fraction of total collected activity in given range interval.

from Ref. 1. The high-energy portion of these two spectra are quite similar, but the one measured here is appreciably broader, with a greater proportion of low energy recoils. A similar effect was noted by Remsberg and Perry[6] in comparing their spectra at 28 GeV with the ones at 2.9 GeV (Ref. 1) and 5.5 GeV.[2]

Cumming *et al.*[1] found that by transforming their data to velocity spectra, the distributions were nearly Gaussian, the only deviation from that form being in the low-velocity region. Accordingly, we have treated our data in the same way, and the velocity spectra at the three angles are shown in Fig. 3 as histograms, with the Gaussian fits as dashed curves. [The units of velocity used are $(\mathrm{MeV}/A)^{1/2}$, obtained from the relation $v = (2E/A)^{1/2}$, with E in MeV.] In making these fits, the lowest velocity point was not included. In addition, the finite resolution of the data was corrected for, using an initial fit to a Gaussian to make the correction. The parameters of these fits are given in Table III; for each angle we list the mean velocity $\langle v_L \rangle$ and the standard deviation $\sigma(v_L)$.

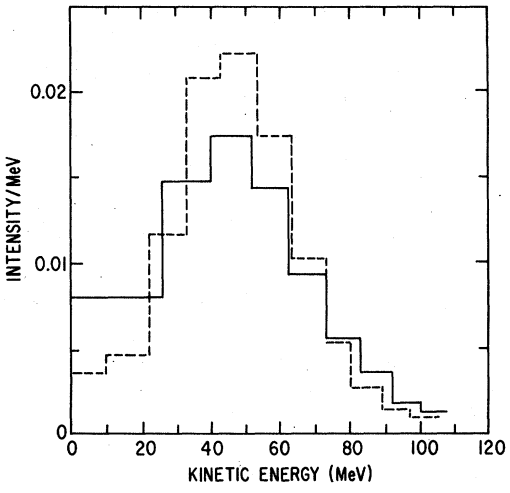

FIG. 2. Kinetic energy distribution for ^{24}Na at a laboratory angle of 90° (solid histogram), in units of intensity per MeV. The dashed histogram shows the corresponding distribution measured at a bombarding energy of 2.9 GeV (Ref. 1).

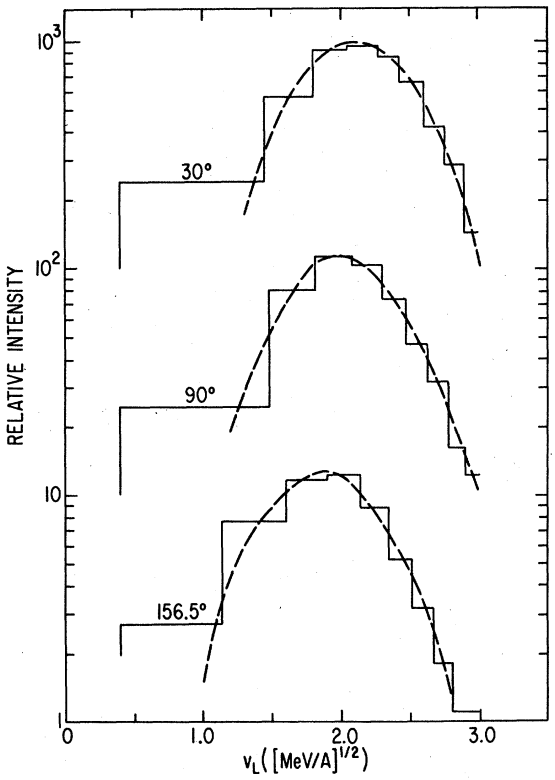

FIG. 3. Velocity distributions for ^{24}Na at the three laboratory angles for which measurements were made. The dashed curves are Gaussian fits to the data, excluding the lowest velocity part.

TABLE III. Mean values and standard deviations of laboratory velocity distributions at different angles.

Laboratory angle θ_L (deg)	$\langle v_L \rangle$ ([MeV/A]$^{1/2}$)	$\sigma(v_L)$ ([MeV/A]$^{1/2}$)
30	2.11 ± 0.05	0.43
90	2.00 ± 0.05	0.41
156.5	1.86 ± 0.05	0.40

IV. MODEL ANALYSIS AND DISCUSSION

In this section we will analyze the experimental results using the two-step reaction model described in the Introduction. As a result of the first step of the reaction, an excited nucleus is formed which is moving with velocity $\vec{v}$ in the laboratory. Let us denote the components of $\vec{v}$ parallel and perpendicular to the beam direction by $v_{\parallel}$ and $v_{\perp}$, respectively. This excited nucleus breaks up, emitting the light fragment at an angle θ with respect to the beam direction and with a velocity in the moving frame of $\vec{V}$. The angular distribution of fragment emission is assumed to be symmetric about 90° to the beam, which is the fundamental assumption of the model, and follows if the two steps are well separated in time. The angular distribution thus can be written as

$$I(\theta) = 1 + b\cos^2\theta . \tag{1}$$

The velocities $v_{\parallel}$, $v_{\perp}$, and V will have distributions also, and there may be correlations between them.

The procedure we shall follow to analyze our data is to obtain initial estimates of $\langle v_{\parallel} \rangle$, $\langle V \rangle$, and b [Eq. (1)], using some simplifying approximations. Then an inverse calculation is carried out, in which we assume distributions in $\vec{v}$ and $\vec{V}$, possible correlations between them, and a value of b, and generate the laboratory velocity and angular distributions for comparison with experiment. This procedure has been successfully used by Cumming and co-workers[17,18] to analyze fission and deep spallation reactions.

The average values of the two velocities can be estimated in a simple way from the mean laboratory velocities at 15° and 156°, in the following way. We first extrapolate the mean velocities at those angles to angles of 0° and 180°, assuming them to be linear in $\cos\theta_L$. Approximate values of $\langle v_{\parallel} \rangle$ and $\langle V \rangle$ are then given by the relations

$$\langle v_{\parallel} \rangle = \tfrac{1}{2}(\langle v_L \rangle_0 - \langle v_L \rangle_{180}) , \tag{2}$$

$$\langle V \rangle = \tfrac{1}{2}(\langle v_L \rangle_0 + \langle v_L \rangle_{180}) . \tag{3}$$

The results of this procedure are $\langle v_{\parallel} \rangle = 0.14$ (MeV/A)$^{1/2}$, $\langle V \rangle = 1.99$ (MeV/A)$^{1/2}$.

By using these average velocities as if they were simple vectors, the laboratory angular distribution can be transformed[19] into the frame moving with velocity $\langle v_{\parallel} \rangle$. The result of such a transformation is shown in Fig. 4 as the points. It is evident that the distribution is indeed symmetric around 90°; the curve in Fig. 4 is Eq. (1) with $b = -0.30$. Thus, even with this approximate analysis, which neglects $v_{\perp}$, distributions in the velocities, and correlations between $\vec{v}$ and $\vec{V}$, we see that the data appear to be consistent with the two-step model.

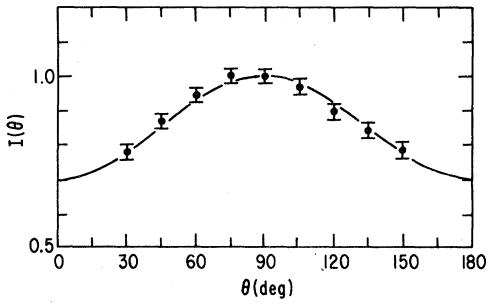

FIG. 4. Angular distribution of ^{24}Na as transformed into the frame moving with respect to the laboratory with a velocity $v_{\parallel} = 0.14$ (MeV/A)$^{1/2}$. The curve is the function $1 - 0.30\cos^2\theta$.

For the inverse calculation of the laboratory distributions from assumed primary distributions, a Monte Carlo technique was used. A distribution of V was chosen and was assumed to be independent of θ. For simplicity, and because the laboratory velocity distributions are very nearly Gaussian, a Gaussian distribution of V was used. For each Monte Carlo event a value of V was selected by means of a random number. The angle θ was chosen from an assumed angular distribution of the form of Eq. (1). Values of $v_{\parallel}$ and $v_{\perp}$ could also be chosen from assumed distributions, but it was found that there was almost no difference between that and simply taking fixed values of these quantities. Therefore fixed values of $v_{\parallel}$ and $v_{\perp}$ were used in the calculations. The azimuthal angle of $v_{\perp}$ was chosen from a uniform distribution.

Addition of the three velocity vectors gives the resultant laboratory velocity v_L and its angle θ_L. Typically, 10^5 events were summed for each parameter set and the resulting angular and velocity distributions compared with the experimental ones. In this way, a "best" set of parameters was found, as well as the limits within which they could be varied without the fit worsening appreciably. This set of parameters is given in Table IV.

Except for $v_{\perp}$, the parameters of the two-step model are determined within rather narrow limits by the data. Comparing Table IV with the approxi-

TABLE IV. Parameters of the two-step model giving the best fit to the experimental data. The units of the velocities are $(\mathrm{MeV}/A)^{1/2}$.

Parameter	Value
$v_{\parallel}$	0.14 ± 0.02
$v_{\perp}$	0.10 ± 0.10
V	2.00 ± 0.04
σ_V	0.41 ± 0.02
b	-0.30 ± 0.02

mate values derived above, it is seen they are virtually identical. This is because the laboratory velocity distributions are relatively narrow and $\langle v_{\parallel} \rangle \ll \langle V \rangle$, so that $\langle V \rangle$ and σ_V are essentially determined by the 90° distribution, while $\langle v_{\parallel} \rangle$ is determined by the change in $\langle v_L \rangle$ with angle. Figure 4 illustrates how the anisotropy parameter is then fairly well determined by the transformed angular distribution.

As noted, $v_{\perp}$ is not very well determined. The data are consistent with $v_{\perp} = 0$, and in fact the curve shown in Fig. 1 was calculated using the parameters in Table III, with $v_{\perp} = 0$. It was found that for $v_{\perp} \leq v_{\parallel}$ there was essentially no change in the calculated distributions. Increasing $v_{\perp}$ to $1.5\, v_{\parallel}$ caused the width of the 90° velocity distribution to increase significantly more than the experimental width. For even larger $v_{\perp}$, the calculated mean velocity at 90° becomes too large. Thus we can only state that $v_{\perp}$ is of the same order of magnitude as, or smaller than, $v_{\parallel}$.

If we compare the values of these parameters at 11.5 GeV with those at 2.9 GeV,[1] we find that $\langle v_{\parallel} \rangle$ is smaller (0.14 compared to 0.20), $\langle V \rangle$ is nearly the same, and σ_V is slightly larger. The most significant change, however, is in the angular distribution, which is forward peaked in the moving system at 2.9 GeV, but symmetric about 90° at 11.5 GeV. Thus the basic assumption of the two-step model is confirmed by the data at 11.5 GeV for this fragmentation product, in contrast to lower energies.

The significance of this fit to the model is open to question, however. At 2.9 GeV, Cumming *et al.*[1] concluded from the forward peaking that the mechanism of formation of ^{24}Na was a rapid one, in which the memory of the beam direction was retained to some extent. At 11.5 GeV one might conclude that the mechanism does proceed in two steps, in which the second step is slow enough that the angular distribution shows no such memory effect. However, it is difficult to rationalize why this change in mechanism should occur with increasing bombarding energy, since one would expect faster time scales at the higher energies.

It is possible that the fit of the present data is fortuitous, in the following sense. The decrease in the thick-target F/B ratio for ^{24}Na with increasing bombarding energy[10,12] above 3 GeV suggests that the trend of the shift in the angular distribution of a light fragment such as ^{24}Na toward more sideward peaking continues above 11.5 GeV. Thus it may be that at still higher energies the data will again deviate from the model, but in the direction of an angular distribution which is higher at 180° than at 0° in the moving frame derived from the velocity distributions. The backward enhancement observed[8] at 400 GeV for some nuclides also suggests this. This is not a definite conclusion, however, since the thick-target F/B ratio depends on the velocity distributions as well as the angular distributions.

As an illustration of this point it is instructive to use the differential measurements of this work to calculate the thick-target recoil parameters, which have been previously determined[12] for ^{24}Na from Au at 11.5 GeV. Consider a recoil emitted from a depth x in the target at an angle θ. It will escape from the target if its range R is greater than the path length to the surface, i.e.,

$$R > x/\cos\theta \,. \tag{4}$$

If we assume a range-velocity relationship of the form

$$R = kV^N \,, \tag{5}$$

as is usually done, then recoils with velocity greater than $V_{\min} = (x/k\cos\theta)^{1/N}$ will escape. Then the fraction escaping in the forward direction from a target of thickness W is

$$F = \frac{2\pi}{\sigma W} \int_0^W dx \int_0^{\pi/2} \sin\theta \, d\theta \int_{V_{\min}}^{\infty} \frac{d^2\sigma}{d\Omega \, dv} dv \,, \tag{6}$$

where σ is the total cross section. The expression for B, the fraction escaping backward, is the same except that the angle integration is from $\pi/2$ to π.

Because the mean velocity is higher in the forward direction, a greater fraction of the recoils will have velocities greater than $V_{\min}$ and will escape. Thus, the thick-target F/B will in general be greater than that for a thin target whenever the mean laboratory velocity is greater at forward angles than at backward ones.

Equation (6) was numerically integrated, using the Gaussian fits to the velocity distributions as a function of angle from Table III and the angular distribution given in Table I. The range-velocity relation was the same as that used in Ref. 12. The results of this calculation were $F/B = 1.48$ and $2W(F+B) = 12.6$ mg/cm^2, for a target thickness $W = 24$ mg/cm^2. The corresponding experimental

values[12] are 1.53 ± 0.03 and 12.7 ± 0.4 mg/cm^2, in excellent agreement. Perhaps the main conclusion from this comparison is that the range-velocity relations for ^{24}Na in Mylar and in gold are consistent with each other.

The mean velocities derived from the thick-target measurements[12] were $\langle v_{\parallel} \rangle = 0.15$ (MeV/A)$^{1/2}$ and $\langle V \rangle = 1.85$ (MeV/A)$^{1/2}$. While the former is in good agreement with the present results, the latter is about 8% smaller. This is a consequence of one of the simplifying approximations used in the thick-target analysis, namely, that the angular distribution in the moving frame is isotropic ($b = 0$). For a sideward-peaked distribution ($b < 0$), the isotropic assumption leads to an underestimation of $\langle V \rangle$. Using the complete equations[20] with $b = -0.3$ gives a $\langle V \rangle$ in better agreement with the present data.

The sideward-peaked angular distributions for light fragments which have been observed recently[6,7] at proton energies above 10 GeV have been confirmed and extended by the present work. The fact that the angular distribution in the laboratory system peaked at about 70° in the 28-GeV experiments[6] led to the suggestion that a nuclear shock wave might be the cause, since that angle was predicted[21] for nucleons and light fragments ejected by such a phenomenon. The conditions for generating a shock wave are expected to become more likely as the projectile energy increases, because of the decreasing opening angle of the energetic secondary particles.

Sideward peaking has also been observed[22] for isotopes of Ba formed from U at 11.5 GeV; both neutron-excess and neutron-deficient isotopes show this feature. At a bombarding energy of 2.2 GeV, however, a forward-peaked angular distribution was observed[17] for neutron-deficient ^{131}Ba formed from U. The change in angular distributions to sideward peaking at high energy thus appears to be a rather general phenomenon and may be the result of a change in the mechanism of energy and momentum transfer to a nucleus by a relativistic hadron. This may be a change from an intranuclear cascade[23] to a coherent interaction[24,25] at highly relativistic energies.

As a result of an intranuclear cascade the excited residual nucleus is moving in the forward direction and its forward velocity and excitation energy are directly related.[12,23] Preferential emission of fragments in the forward direction then results from an extensive cascade in which large amounts of energy and momentum are transferred.

At highly relativistic energies, however, there is considerable evidence that such cascading is much less important. For example, the multiplicity of charged particles emerging at small angles in a hadron-nucleus collision is independent of the mass of the nucleus,[26,27] indicating the lack of cascading of these particles. In the coherent models[24,25] the projectile is considered to interact collectively with the nucleons which lie in its path, as an effective target resulting from the Lorentz contraction of the nucleus as seen by the projectile. As a result of the interaction, an excited hadronic state is formed, which does not decay to its final multiparticle state until after it has left the nucleus. Therefore, these secondary particles do not participate in the intranuclear cascade.

The suggestion has been made[13,28] that this type of collective interaction might account for the sideward peaking under discussion. In a nearly central collision of the projectile with a heavy nucleus, the participating nucleons are rapidly ejected from the nucleus in the forward direction, leaving the nucleus with a longitudinal "tunnel" of depleted nuclear matter. If the nucleus should split into two fragments as a result of this process, their Coulomb repulsion will cause them to separate, and they will tend to be emitted at 90° to the beam. The present data cannot test the validity of such a model, since it is an inclusive experiment, i.e., a single product is observed, inclusive of all possible additional products. Experiments in which correlations between coincident fragments are measured should provide more definitive information on the importance of such a mechanism in the formation of light nuclear fragments, such as ^{24}Na.

V. SUMMARY AND CONCLUSIONS

The formation of a typical light nuclear fragment ^{24}Na from a heavy target Au by 11.5-GeV protons has been studied by measuring the angular distribution and the range distributions at 3 angles. The angular distribution has a peak at a laboratory angle of $\theta_L \approx 70°$ and is quite different from the forward-peaked distribution observed[1] at 2.9 GeV. It is similar to those observed[6] for $Z = 11$ (Na) fragments at 28 GeV from targets of Au and U.

The velocity distributions are relatively narrow and are well approximated by Gaussian distributions, with a low-velocity tail. The mean velocity is a function of laboratory angle, decreasing from 2.11 (MeV/A)$^{1/2}$ at 30° to 1.86 (MeV/A)$^{1/2}$ at 156.5°. When these distributions are analyzed in terms of the two-step model, a satisfactory fit is obtained with a single velocity distribution in a moving frame and an angular distribution in that frame which is symmetric about 90°. The velocity of the moving frame with respect to the laboratory is 0.14 (MeV/A)$^{1/2}$ in the beam direction; a possible component at 90° to the beam direction may be as

large as 0.20 $(\mathrm{MeV}/A)^{1/2}$, but the data are consistent with a zero component. When transformed to that moving frame, the angular distribution is symmetric about 90° and has a maximum at 90°.

These results apparently indicate the validity of the two-step model, implying that the breakup into the light fragment occurs after memory of the initial, fast cascade step is lost, i.e., it is a slow process. If the fragmentation process is a fast one at 2.9 GeV, it seems unlikely that it would change to a slow one at 11.5 GeV. Thus, either the interpretation of the 2.9-GeV data is in error and fragmentation is not a fast process at that energy or the agreement with the two-step model at 11.5 GeV is accidental and does not imply a slow process. There is evidence that the angular distribution becomes even less forward peaked at still higher energies. The latter data lead to a transformed angular distribution in the moving frame which is again not symmetric about 90° and is actually enhanced in the backward direction in disagreement with the two-step model.

Thus, it may well be that the fragmentation mechanism is indeed a fast one at all energies above about 2.9 GeV, but that the change in the angular distribution from forward to sideward peaking introduces a fortuitous agreement with the two-step model analysis at 11.5 GeV.

ACKNOWLEDGMENTS

This work was supported by the Division of Nuclear Physics of the U. S. Department of Energy. We are grateful to the operating crews of the Argonne ZGS for their kind cooperation during the experiments.

[1]J. B. Cumming, R. J. Cross, Jr., J. Hudis, and A. M. Poskanzer, Phys. Rev. 134, B167 (1964).
[2]A. M. Poskanzer, G. W. Butler, and E. K. Hyde, Phys. Rev. C 3, 882 (1971).
[3]E. K. Hyde, G. W. Butler, and A. M. Poskanzer, Phys. Rev. C 4, 1759 (1971).
[4]R. G. Korteling, C. R. Toren, and E. K. Hyde, Phys. Rev. C 7, 1611 (1973).
[5]G. D. Westfall, R. G. Sextro, A. M. Poskanzer, A. M. Zebelman, G. W. Butler, and E. K. Hyde, Phys. Rev. C 17, 1368 (1978).
[6]L. P. Remsberg and D. G. Perry, Phys. Rev. Lett. 35, 361 (1975).
[7]D. R. Fortney and N. T. Porile, Phys. Lett. 76B, 553 (1978).
[8]N. T. Porile, D. R. Fortney, S. Pandian, R. A. Johns, T. Kaiser, K. Wielgoz, T. S. K. Chang, N. Sugarman, J. A. Urbon, D. J. Henderson, S. B. Kaufman, and E. P. Steinberg, Phys. Rev. Lett. 43, 918 (1979).
[9]K. Beg and N. T. Porile, Phys. Rev. C 3, 1631 (1971).
[10]S. B. Kaufman and M. W. Weisfield, Phys. Rev. C 11, 1258 (1975).
[11]O. Scheidemann and N. T. Porile, Phys. Rev. C 14, 1534 (1976).
[12]S. B. Kaufman, E. P. Steinberg, and M. W. Weisfield, Phys. Rev. C 18, 1349 (1978).
[13]S. Biswas and N. T. Porile, Phys. Rev. C 20, 1467 (1979).
[14]C. R. Rudy, N. T. Porile, and S. B. Kaufman, Nucl. Instrum. Methods, 138, 19 (1976).
[15]Supplied by Carlo Erba, Milan, Italy.
[16]L. C. Northcliffe and R. F. Schilling, Nucl. Data Sect. A7, 233 (1970).
[17]V. P. Crespo, J. B. Cumming, and A. M. Poskanzer, Phys. Rev. 174, 1455 (1968).
[18]V. P. Crespo, J. B. Cumming, and J. M. Alexander, Phys. Rev. C 2, 1777 (1970).
[19]J. B. Marion, T. I. Arnette, and H. C. Owens, Oak Ridge National Laboratory Report No. ORNL-2574, 1959 (unpublished).
[20]L. Winsberg and J. M. Alexander, *Nuclear Chemistry*, edited by L. Yaffe (Academic, New York, 1968), Vol. I, p. 340.
[21]A. E. Glassgold, W. Heckrotte, and K. M. Watson, Ann. Phys. (N.Y.) 6, 1 (1959).
[22]N. T. Porile, S. Pandian, H. Klonk, C. R. Rudy, and E. P. Steinberg, Phys. Rev. C 19, 1832 (1979).
[23]K. Chen, Z. Fraenkel, G. Friedlander, J. R. Grover, J. M. Miller, and Y. Shimamoto, Phys. Rev. 166, 949 (1968).
[24]G. Berlad, A. Dar, and G. Eilam, Phys. Rev. D 13, 161 (1976).
[25]Meng Ta-Chung and E. Moeller, Phys. Rev. Lett. 41, 1352 (1978).
[26]W. Busza, in *High-Energy Physics and Nuclear Structure-1975* (American Institute of Physics, New York, 1975), p. 211.
[27]C. Halliwell, J. E. Elias, W. Busza, D. Luckey, L. Votta, and C. Young, Phys. Rev. Lett. 39, 1499 (1977).
[28]B. D. Wilkins, S. B. Kaufman, E. P. Steinberg, J. A. Urbon, and D. J. Henderson, Phys. Rev. Lett. 43, 1080 (1979).